Experimental and Numerical Investigation of the SBS-Threshold Increase in an Optical Fiber by Applying Strain Distributions

J. M. Chavez Boggio, J. D. Marconi, and H. L. Fragnito

***Abstract*—We study, experimentally and numerically, the increase of the stimulated Brillouin scattering (SBS) threshold in dispersion-shifted fibers (DSFs) by applying three different tensile-strain distributions. The best results are obtained with a 40-step stair-ramp distribution, for which we demonstrate a 8-dB SBS threshold increase in a 580-m DSF. The Brillouin frequency is observed to shift as a function of the strain at a rate of 0.464 GHz/%. We discuss the potentials and drawbacks of this technique for application in nonlinear devices.**

***Index Terms*—Brillouin threshold, nonlinear fiber optics, stimulated Brillouin scattering (SBS), strain.**

I. Introduction

STIMULATED Brillouin scattering (SBS) is a process in which a laser interacts with a backscattered Stokes wave through the intermediary of an acoustic wave, producing the attenuation of the pump and the amplification of the Stokes wave. SBS is an undesirable effect in several applications of optical fibers. In metropolitan-area wavelength division multiplexing (WDM) networks, for example, SBS limits seriously the total amount of optical power that can be transmitted through a single fiber [1]–[3]. Another application where SBS represents a serious limitation is in the field of fiber-optic parametric devices [4]–[8]. In these devices, one or two strong pumps amplify, by four-wave mixing (FWM), a weak signal and generate an idler wave, which can be used for wavelength conversion or optical signal processing in optical networks. The SBS, if not completely suppressed, induces random variations of the pump power that are transferred to the signal as an intensity noise degrading the signal performance. Two techniques permit an increase of the SBS threshold:

1) by broadening the linewidth of the laser by phase or frequency modulation; or
2) by broadening the Brillouin-gain bandwidth by varying the frequency of the acoustic wave along the fiber.

The first technique permits a raise of the SBS threshold by up to 17 dB if the laser is broadened by 8.4 GHz [9]. However, this spectral broadening combined with fiber dispersion will give rise to timing jitter. Even in dispersion-compensated systems, third-order dispersion will produce a small amount of timing jitter that should limit the transmitted bit rate $\times$ length [3]. Technique 2) can be implemented by varying the core radius (maximum threshold increase reported was 4.8 dB) [10], [11], dopant concentration (7-dB increase) [11]–[13], or temperature (4.8-dB increase) [14], [15]. In [16], a fiber cable structure with tensile and compressive strains that resulted in a 7-dB SBS threshold increase was reported. In [17], we recently demonstrated a 7.3-dB SBS threshold increase by applying strain distributions in 500 m of a dispersion-shifted fiber (DSF).

In this paper, we report an experimental and numerical study of the SBS power threshold increase by applying three different strain distributions along a DSF: rectangular-periodic, triangular-periodic, and stair-ramp distributions. In Section II, we use a simple and accurate model to calculate the increase of the Brillouin threshold in a fiber with nonuniform Brillouin-frequency-shift distributions along its length. In Section III, the experimental setup is described, and in Section IV, we present our experimental results, which are compared with the numerical ones. We obtained a maximum of 8 dB in the SBS power threshold increase with the application of a 40-step stair-ramp distribution in a 580-m length DSF. In Section V, we discuss the advantages of broadening the Brillouin-gain bandwidth by inducing tensile strains and comparing with other schemes. Finally, in Section VI, we present our conclusions.

II. SBS Threshold in Optical Fibers: Numerical Results

Brillouin scattering results from the light scattering by acoustic waves. Thermally excited acoustic waves produce a periodic modulation of the refractive index and the light is diffracted by this moving grating, generating a frequency-shifted Stokes light wave. The interference of the incident light wave with the Stokes wave contains a frequency component equal to the frequency of the sound wave. Thus, the beating of the laser wave with the sound wave tends to reinforce the Stokes wave and the beating of the laser wave with the Stokes wave tends to reinforce the sound wave by the physical mechanism of electrostriction (the tendency of materials to become denser where the intensity of electric field is stronger) [18]. Spontaneous Brillouin scattering occurs when the light scattering is mainly due to thermally excited acoustic waves. The SBS occurs when the process of electrostriction is strong enough in a way that the acoustic and Stokes waves mutually reinforce each other to generate an exponential growth of the

Manuscript received June 8, 2004; revised June 21, 2005. This work was supported by Fapesp, Pronex, CAPES and CNPq.

The authors are with the Optics and Photonics Research Center, Unicamp—IFGW, 13083-970 Campinas, SP, Brazil (e-mail: jmchavez@ifi.unicamp.br).

Digital Object Identifier 10.1109/JLT.2005.856226

amplitude of the Stokes wave. To model the evolution of the Stokes wave by SBS, we consider a pump laser at frequency $\nu_{\rm p}$, with power $P_{\rm p}$, which interact with a counterpropagating Stokes wave with power $P_{\rm S}$ at $\nu_{\rm S}$. The coupled equations for the pump and the Stokes waves under steady-state conditions of the SBS are [18]

$$\frac{{\rm d}P_{\rm P}(z)}{{\rm d}z} = \frac{-g(\nu,z)P_{\rm S}P_{\rm P}}{A_{\rm eff}} - \alpha P_{\rm P}(z) \tag{1a}$$

$$\frac{{\rm d}P_{\rm S}(z)}{{\rm d}z} = \frac{-g(\nu,z)P_{\rm P}P_{\rm S}}{A_{\rm eff}} + \alpha P_{\rm S}(z) \tag{1b}$$

where z is distance along the fiber, $g(\nu,z)$ is the local SBS gain coefficient, $\nu = \nu_{\rm p} - \nu_{\rm S}$, α is the attenuation coefficient, and $A_{\rm eff}$ is the effective area. The Brillouin-gain spectrum is observed to be Lorentzian

$$g(\nu,z) = g_0 \frac{\left(\frac{\Delta\nu_{\rm B}}{2}\right)^2}{\left(\frac{\Delta\nu_{\rm B}}{2}\right)^2 + (\nu - \nu_{\rm B}(z))^2} \tag{2a}$$

$$g_0 = \frac{\gamma_{\rm e}^2}{nc\lambda_{\rm p} v_{\rm A} \rho_0 \Delta\nu_{\rm B}} \tag{2b}$$

where $\Delta\nu_{\rm B}$ is the Brillouin linewidth, g_0 ($\approx 2.5\ 10^{-11}$ m/W in optical fibers [19]) is the peak value of the gain coefficient, $\nu_{\rm B}(z)$ is the Brillouin frequency at z, $\gamma_{\rm e}$ is the electrostrictive constant, ρ_0 is the mean density of the medium, and $v_{\rm A}$ is the velocity of the (longitudinal) acoustic waves. In general, the velocity of acoustic waves can vary with z and the Brillouin frequency is given by

$$\nu_{\rm B}(z) = \frac{2nv_{\rm A}(z)}{\lambda_{\rm p}}. \tag{3}$$

The velocity of sound depends on the Young's modulus $E_0(z)$, the Poisson's ratio $\kappa(z)$, and the density $\rho(z)$

$$v_{\rm A}(z) = \sqrt{\frac{E_0(1-\kappa)}{\rho(1+\kappa)(1-2\kappa)}}. \tag{4}$$

We consider that the pump is not depleted by transferring energy to the backscattered wave, thus, $P_{\rm p}(z) = P_{\rm p}(0)\exp(-\alpha z)$. From (1), we obtain

$$P_{\rm S}(0) = P_{\rm S}(L)\exp\left(-\alpha L + G(\nu)\right) \tag{5a}$$

$$G(\nu) = \frac{P_{\rm p}}{A_{\rm eff}} \int_0^L g(\nu,z)\exp(-\alpha z){\rm d}z \tag{5b}$$

where L is the fiber length and G is the effective gain factor.

In a uniform fiber, $v_{\rm A}$ is constant along the fiber, and from (2a) and (5b), the maximum effective gain (for $\nu = \nu_{\rm B}$) is $G_0 = P_{\rm p} g_0 L_{\rm eff}/A_{\rm eff}$, where $L_{\rm eff} = (1-\exp(-\alpha L))/\alpha$ is the effective interaction length. Replacing into (5a), we obtain

$$P_{\rm S}(0) = P_{\rm S}(L)\exp\left(-\alpha L + \frac{P_{\rm p}(0) g_0 L_{\rm eff}}{A_{\rm eff}}\right). \tag{6}$$

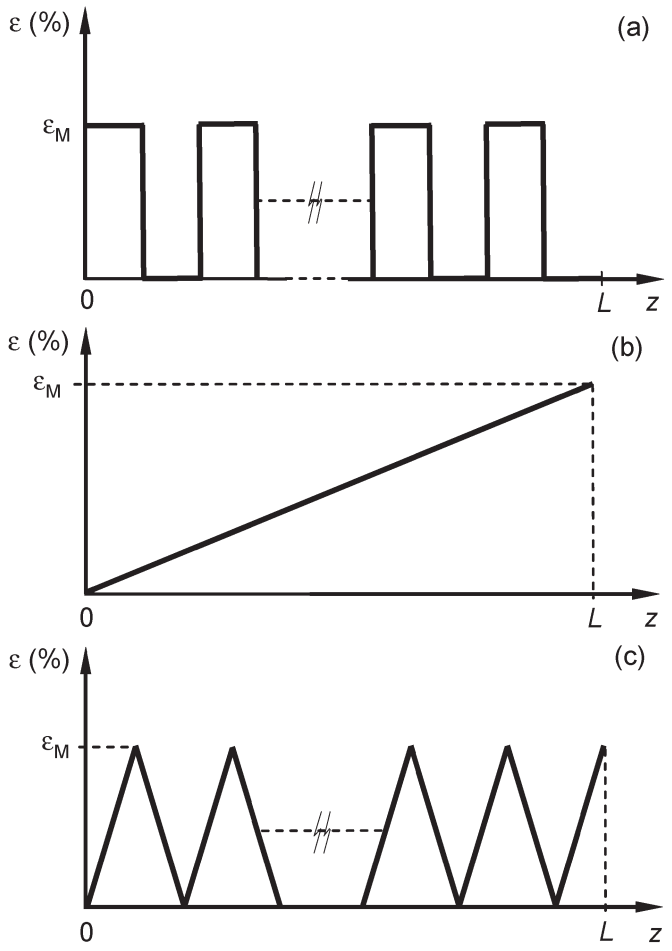

Fig. 1. Strain distribution used in the simulations. (a) Rectangular periodic. (b) Stair ramp. (c) Triangular periodic.

It is known empirically that the threshold condition for SBS occurrence is obtained when G exceeds some threshold value, which is typically of the order of 20 [20]. In an uniform fiber, the SBS power threshold is $P_{\rm SBS} \cong 20A_{\rm eff}/g_0 L_{\rm eff}$. On the other hand, in a nonuniform fiber, where $\nu_{\rm B}$ varies along z, the maximum effective gain factor $G_{\rm MAX}(\nu_{\rm MAX}) < G_0$, and the SBS power threshold is

$$P'_{\rm SBS} = \frac{20A_{\rm eff}}{\int_0^L g(\nu_{\rm MAX},z){\rm d}z}. \tag{7}$$

The SBS threshold increase in decibel units is then written as

$$P_{\rm inc} = -10\log\left[\frac{1}{L_{\rm eff}}\int_0^L \frac{{\rm d}z}{1 + \frac{4(\nu_{\rm MAX} - \nu_{\rm B}(z))^2}{\Delta\nu_{\rm B}^2}}\right]. \tag{8}$$

By solving (8) numerically, we can calculate the threshold increase for arbitrary strain distributions. In Fig. 1, we show the three distributions considered in our study: rectangular periodic, stair ramp, and triangular periodic. The parameters we

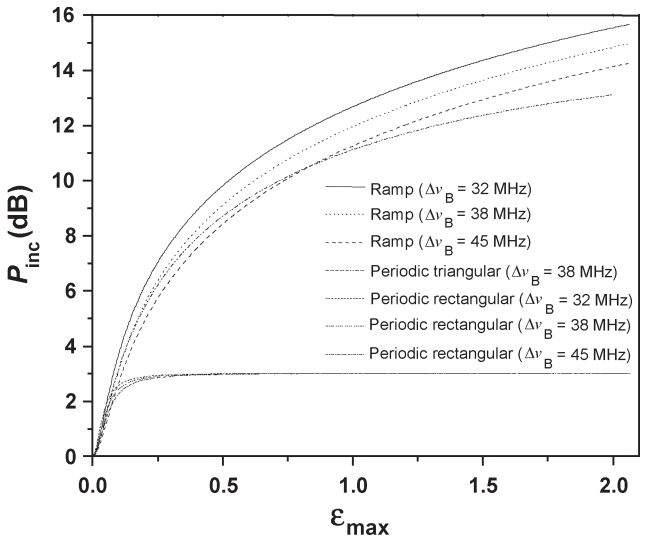

Fig. 2. SBS power threshold increase as a function of $\varepsilon_{\rm M}$ for the three strain distributions shown in Fig. 1. These distributions were constructed by dividing the fiber length into 400 segments. In the stair-ramp and rectangular-periodic cases, three different values of $\Delta\nu_{\rm B} = 32$, 38, and 45 MHz were used.

used to solve (8) were: $L_{\rm eff} = L = 580$ m, $\nu_{\rm MAX} = 10.5$ GHz, and $\nu_{\rm B}(z) = \nu_{\rm MAX} + \beta\varepsilon(z)$, where

$$\beta = \frac{\partial \nu_{\rm B}}{\partial \varepsilon} = 0.464 \text{ GHz}/\% \tag{9}$$

is the strain coefficient of the Brillouin frequency and $\varepsilon = 100\Delta l/l_0$ is the strain applied in the fiber (l_0 is the initial length and Δl the elongation). These parameters were obtained from our measurements (see Section IV). An important point is what Brillouin linewidth to plug into (8). It is well know that the Brillouin linewidth in single-mode optical fibers vary from $\Delta\nu_{\rm B} \sim 10$ to $\sim$ 150 MHz depending on the input power of the pump laser and on the numerical aperture of the fiber [21]. In our simulations, we considered that $\Delta\nu_{\rm B}$ at the SBS threshold is in the range 32–45 MHz. In the Appendix, we discuss the consistency of considering these values. In Fig. 2, we show the SBS power threshold increase for the three distributions as a function of the maximum applied strain $\varepsilon_{\rm M}$. The rectangular-periodic distribution produces the smallest SBS threshold increase as it saturates at about 3 dB. The stair-ramp and the triangular-periodic distributions show a monotonic increasing behavior with strain, though the stair-ramp distribution has a better performance than the triangular. For the case of the rectangular-periodic and stair-ramp distributions, we considered three values of $\Delta\nu_{\rm B} = 32$, 38, and 45 MHz. Note that in the rectangular-periodic distribution, the different values of $\Delta\nu_{\rm B}$ produce slightly different values in the SBS power threshold increase only for strains up to 0.5%. For higher strains, the different values of $\Delta\nu_{\rm B}$ produce the same saturation behavior at 3 dB. In the stair-ramp case, the different values of the Brillouin linewidth give three curves clearly separated. However, the difference in the SBS power threshold increase between $\Delta\nu_{\rm B} = 32$ MHz and 45 MHz is almost constant ($\sim$ 1.3 dB) for strains higher than 0.2%, and lower than that for strains from 0% to 0.2%.

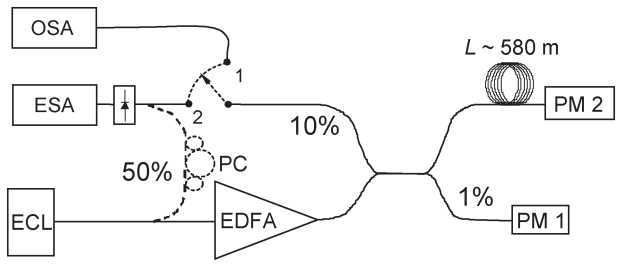

Fig. 3. Experimental setup. PM: Power meter.

III. Experimental Setup

The experimental setup is shown in Fig. 3. The pump was an external cavity laser (ECL) with a nominal linewidth of 120 kHz, boosted by an Erbium-doped fiber amplifier (EDFA) providing up to 2-W output power. Measurements were performed in 580 and 500 m of DSF. The input and the output pump power were measured using power meters PM1 and PM2, respectively. The backscattered light can be measured using either an optical spectrum analyzer (OSA, with resolution bandwidth of 0.01 nm) or an electrical spectrum analyzer (ESA). In the ESA case, dashed lines indicate the light path, where we inserted a 50% tap coupler to combine the backscattered light with a sample of the laser in a photodiode. The polarization controller permitted us to enhance the beat of the two waves.

In our experiments, we induced a tensile strain by stretching the fiber from an initial length l_0 to $l_0 + \Delta l$. The scheme of the system used to stretch the fiber is shown in Fig. 4. Our system consisted of 80 acrylic grips arranged in four groups of 20, where each group is mounted on a rigid structure of aluminum. Half of the grips were mounted in mechanical translators that allowed us to stretch different segments of fiber independently, with a maximum elongation of 10 cm. The grips were designed to contain more than just one fiber, with the objective of maximizing the quantity of fiber in the setup. Thus, 30 pairs of grips have four fibers between them and ten pairs have six fibers, giving 180 segments of fiber with $l_0 \approx 2.9$ m.

In our system, the fiber in the curves between the two arms (11% of the total fiber length) does not suffer strain. This unstretched fiber implies that the limit on the maximum possible power increase of SBS threshold, which we estimated using the theory in Section II, is 10 dB. To minimize its impact and to maximize the broadening of the Brillouin spectrum, the other 89% of fiber was initially elongated by 3 mm in the case of the triangular distribution and by 4.5 mm in the stair-ramp distribution. In this way, we improve the efficiency of our system by separating the Brillouin frequencies of the stretched and the unstretched fibers. Fig. 5(a) and (b) shows the experimental triangular and stair-ramp strain distributions, respectively. These are slightly different relative to the ideal distributions shown in Fig. 1. The stair-ramp distribution was made with 40 strain steps, where in each successive step Δl was increased by $\sim$ 0.4 mm. The triangular distribution was made of four strain steps and a total of six and a half periods.

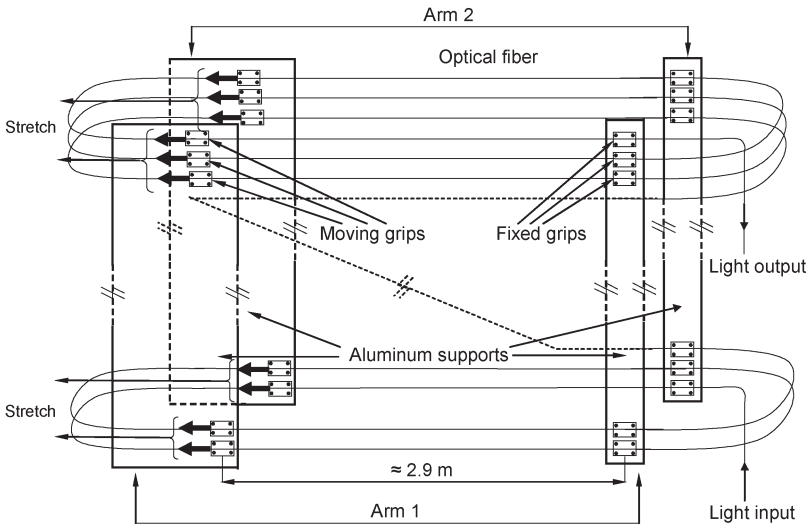

Fig. 4. Scheme of the system to stretch the fiber. The 40 pairs of grips permitted us to construct a rectangular, triangular, and stair-ramp distribution with 40 strain steps.

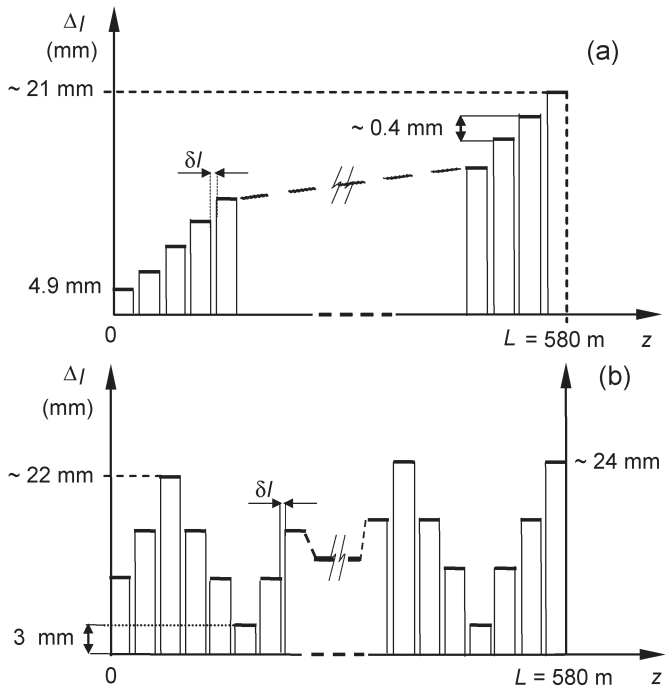

Fig. 5. Deformation distributions used in the experiments (for clarity, we show Δl instead of ε). (a) Stair-ramp strain distribution made with 40 steps. Each step contains four or six fibers of $l_0 \sim 2.9$ m (Δl was increased by 0.4 mm after successive steps). (b) Periodic triangular distribution with four strain steps in six and a half periods. In our setup, the last period was ~ 1 mm more stretched than the other five.

IV. Results

A. Rectangular-Periodic Distribution

Fig. 6(a) shows the measured backscattered power versus input pump power using the two-step periodic strain configuration shown in Fig. 1(a) constructed in 500 m of DSF, for strain values varying from $\varepsilon = 0$ to $\varepsilon = 0.36\%$. The pump was located at $\lambda_{\rm p} = 1570$ nm. Note that increasing the strain up to $\varepsilon = 0.26\%$, the backscattered power decreases, but above that point, increasing the strain does not reduce SBS. We consider that the SBS power threshold $P_{\rm SBS}$ is the condition where the backscattered power begins to rise above the extrapolated spontaneous backscattering power line (i.e., when the exponential growth of the Stokes wave due to electrostriction is larger than linear growth of the Stokes wave due to thermal acoustic waves). Therefore, $P_{\rm SBS} = 15$ dBm and $P_{\rm SBS} = 18$ dBm for $\varepsilon = 0$ and $\varepsilon = 0.26\%$, respectively. Thus, the maximum increase in the SBS threshold was 3 dB for this configuration. In Fig. 6(b), we show the Brillouin spectra for the different strains. Note that for $\varepsilon > 0.09$, the measured spectra show a double-peak structure. For $\varepsilon > 0.21$, the two peaks are well separated and do not vary in amplitudes. From these spectra, we calculate the strain coefficient of the Brillouin frequency as being $\beta = 0.464$ GHz/% (or 0.016 GHz/mm). The normalized slope coefficient $C = \beta/\nu_{\rm B}(0)$ gives 4.4, similar to previously reported coefficients: 4.7 in [22] and 4.4 in [23]. Fig. 6(c) shows the comparison between the measured values and the calculated ones. The agreement is quite good for $\varepsilon \geq 0.2$. Clearly, the saturation behavior observed in Fig. 6(a) and (c) occurs when the Brillouin peaks in Fig. 6(b) are completely separated.

B. Triangular-Periodic and Stair-Ramp Distributions

Fig. 7 shows the backscattered power versus the input power for the 40-step stair-ramp and the triangular-periodic strain distributions with pump at $\lambda_{\rm p} = 1554$ nm. We obtained an increase in the SBS threshold of ~ 8 dB and ~ 7.8 dB, respectively. These are the largest measured values of SBS threshold increase by varying the acoustic frequency along the fiber. For the strain values used in these distributions, the setup introduced a very small amount of additional loss, which within the error margin of our measurements was observed to be < 0.1 dB. In the inset of Fig. 7(a) and (b), we show the backscattered light spectra for these distributions. The peaks in the stair-ramp spectrum are distributed over 320 MHz, while in the triangular-distribution spectrum, there are five peaks distributed over 370 MHz. The peak at 10.5 GHz is due to the unstretched fiber. The distribution of the peaks in these spectra

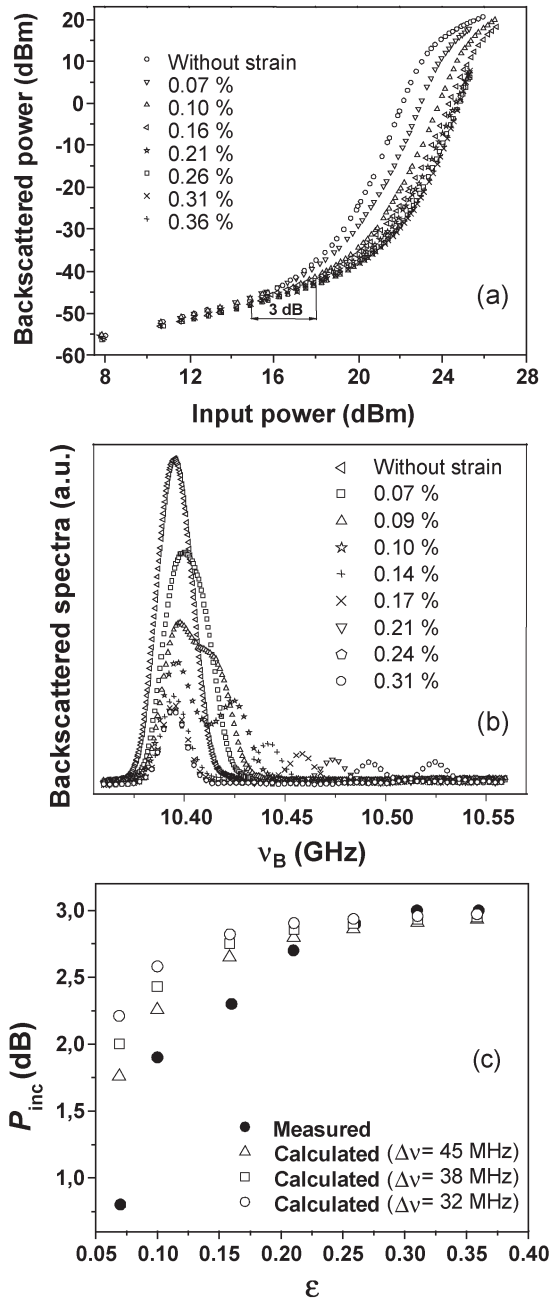

Fig. 6. (a) Backscattered power as a function of the input pump power for the periodic rectangular distribution for various ε_{M}. (b) Backscattered power spectra measured for various ε_{M}. (c) SBS power threshold increase as a function of ε_{M}. Solid circles: Measured, open triangles, squares, and circles: Simulated for $\Delta\nu_{\mathrm{B}} = 32$, 38, and 45 MHz, respectively.

deviates from the applied strain quoted in Fig. 5(a) and (b). We observed that as the fibers were progressively strained at different values of ε, the aluminum bar tilted slightly for the segments where ε was large, thus affecting the strain in all the other segments. In addition, we detected a slight sliding from the grips of some segments of fiber for large ε. For this reason, in the spectrum of the triangular distribution, the central peak is larger and the peaks are not equally spaced. Also, the peak on the right extreme of the spectrum of the ramp distribution appears isolated from the continuous one obtained in the central part. However, for the parameters used in these configurations,

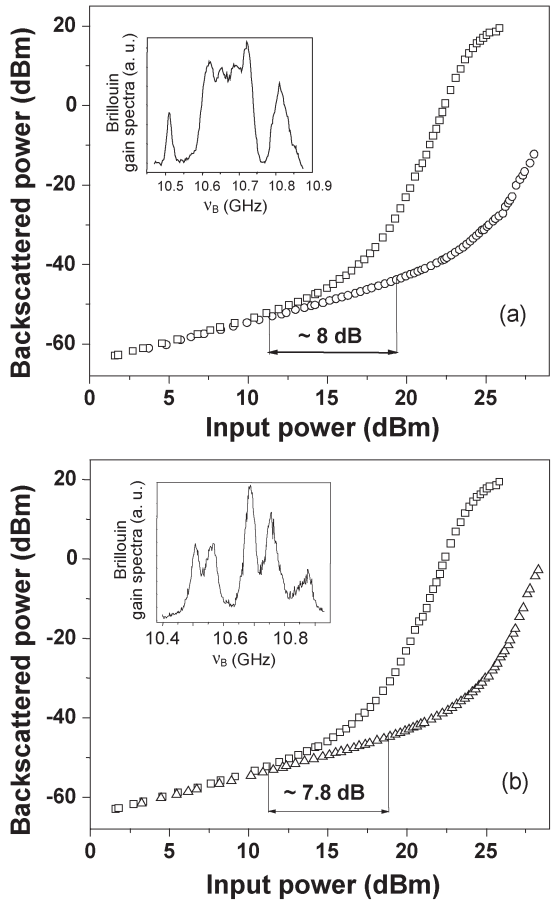

Fig. 7. Backscattered power versus input pump power for (a) stair-ramp distribution. Squares: Without strain; circles: Stair-ramp strain. (b) Triangular-periodic distribution. Squares: Without strain; triangles: Triangular-periodic strain. Insets: Backscattered power spectra.

we calculated P_{inc} from (8) and obtained discrepancies of the order of 0.5 and 0.3 dB for the ramp and the triangular distribution, respectively.

V. Discussion and Comparison With Other Schemes

The maximum broadening of the Brillouin-gain bandwidth that is achievable with tensile strains is related to the fiber breaking point. In our experiments, the strains we applied were limited to $\varepsilon_{\mathrm{M}} = 0.82\%$ due to the robustness of our aluminum structure and the way that the grips fixed the fibers. By improving these structures or the grips, we should be able to do experiments with up to 2% or 3% strains without damaging the DSF or induce fiber loss.

On the other hand, tensile strains also change the zero-dispersion wavelength of the fiber. With the method described in [24], we observed that λ_0 increases linearly with ε with slope

$$\frac{\partial \lambda_0}{\partial \varepsilon} = 4.6\ \mathrm{nm}/\%. \tag{10}$$

Thus, applying a ramp strain distribution with $\varepsilon_{\mathrm{M}} = 3\%$, the Brillouin-gain spectrum will broaden up to 1400 MHz (and the SBS threshold will increase by 17 dB), but the λ_0 will spread in a range of 13.8 nm. This induced variation of λ_0 is a burden for

applications in parametric devices. It is well known that large variations of λ_0 reduce the FWM efficiency in these devices and give rise to a smaller parametric gain [25]. However, other schemes for increase of SBS threshold will induce a stronger variation of λ_0. For example, to produce a broadening of 1400 MHz in the Brillouin-gain spectrum, it would be necessary to raise the fiber temperature by more than 1000 °C, and the resulting variation of the λ_0 will be up to 72 nm, which is 5.2 times larger than with the strain scheme.

To maintain the chromatic dispersion nearly constant and simultaneously increase the SBS threshold, the dopant concentration and core radii were judiciously varied along the fiber, as reported in [11] . Nevertheless, this scheme is complex and expensive and resulted in only 4.5 dB of SBS power threshold increase.

VI. Conclusion

The effect of tensile-strain distributions along the length of an optical fiber on SBS threshold was experimentally and numerically investigated. It is shown that by applying only $\varepsilon = 0.26\%$ tensile strain in a simple rectangular two-step configuration, we are able to obtain an SBS power threshold increase of 3 dB. Larger strains do not reduce the SBS with this configuration. By applying strains evenly divided in more steps, we demonstrate an 8-dB SBS threshold increase in a 580-m DSF for a maximum strain of $\sim 0.72\%$ in the last step. It should be noted that the maximum strain was limited by the robustness of the aluminum structure in our setup and the way that the grips fixed the fibers. With an improved setup, it should be possible to stretch the fiber up to $\varepsilon_{\rm M} = 3\%$ and obtain an increase of the SBS threshold of 17 dB, comparable with phase-modulation schemes. The zero-dispersion wavelength is observed to shift, as a function of the strain, at a rate of 4.6 nm/%. For applications in parametric devices, the induced λ_0 variation should distort the gain spectrum. On the other hand, for metropolitan network applications, the induced reduction of FWM efficiency could permit the transmission of more WDM channels.

Appendix
Brillouin Linewidth in the Threshold Condition

The power threshold for the occurrence of SBS can be defined as the condition where the backscattered SBS power begins to rise above the extrapolated spontaneous backscattering power line; in other words, when the scattering of the light with the acoustic waves induced by electrostriction is stronger than the scattering with the thermally excited acoustic waves. Note that (8) is valid only for the regime of SBS, i.e., when the phenomenon of electrostriction leads to an exponential growth of the Stokes wave [see (5)]. In order to know what Brillouin linewidth to plug into (8), we have measured $\Delta\nu_{\rm B}$ as a function of the pump power entering into the 580-m DSF. Fig. 8 shows our results. For comparison purposes, we also show the backscattered power in decibel units versus input pump power in linear units in order to determine, with the best accuracy, the threshold condition. The stimulated regimen starts

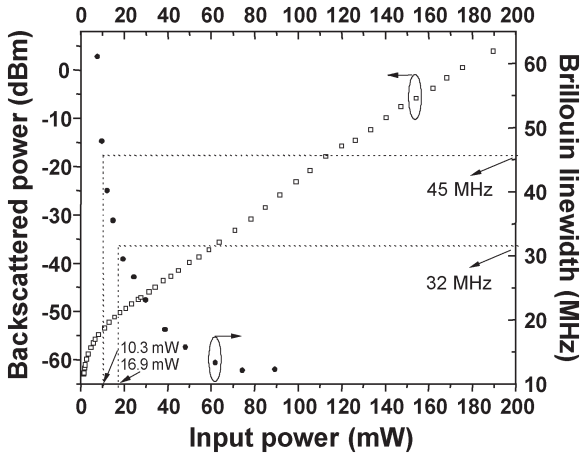

Fig. 8. Brillouin linewidth and backscattered power as a function of the input pump power. Equation (8) is valid for pump powers $P_{\rm p} \geq P_{\rm SBS}$. The narrowing linewidth observed is a phenomenon known as gain narrowing.

when backscattered power in decibel units is proportional to the input pump power in linear units. Thus, we find $P_{\rm SBS}$ around 10–17 mW, giving a $\Delta\nu_{\rm B} = 32{-}45$ MHz.

Note that the Brillouin linewidth varies from $\sim$ 62 MHz for low power values ($P_{\rm p} \cong 9$ dBm) to $\sim$ 13 MHz (for $P_{\rm p} \cong 21$ dBm). The $\Delta\nu_{\rm B}$ values are quite different than the expected Brillouin linewidth due to the damping of the acoustic wave owing to its viscosity ($\sim$ 17 MHz). This extra inhomogeneous broadening can be attributed to random variations of dopant type and concentration, fiber geometry, and to guidance effects. A way of estimating the level of random variations of dopant type and concentration and fiber geometry (core radius), is through the measurement of the variation of λ_0, which were estimated to be smaller than 0.1 nm in our fiber, indicating high uniformity of the mentioned parameters. Thus, waveguide-induced inhomogeneous spectral broadening should be responsible for the observed $\Delta\nu_{\rm B}$ values [21]. The inhomogeneously broadened spontaneous Brillouin scattering can be expressed approximately as $\Delta\nu_{\rm B} \cong [\Delta\nu_{\rm B0}^2 + (v_{\rm A}^2({\rm NA})^4/\lambda^2 n_{\rm co}^2)]^{1/2}$, where $\Delta\nu_{\rm B0} \cong 17$ MHz is the homogeneous Brillouin linewidth, NA ($\cong 0.15$ in our DSF) is the numerical aperture of the fiber, n is the refractive index, and $v_{\rm A}$ is the acoustic waves' velocity. With these values, we obtain $\Delta\nu_{\rm B} \cong 100$ MHz, which should be the Brillouin linewidth for very low power values, in agreement with the range of the measured $\Delta\nu_{\rm B}$.

Acknowledgment

The authors would like to gratefully acknowledge J. B. Rosolem, A. A. Juriollo, and J. C. Said, from Fundação CPqD, and R. Braga from Xtal Fiber Core, for the loan of equipment used in this investigation.

References

[1] K. H. Yla-Jarkko, S. Alam, and A. B. Grudinin, "Achieving long repeaterless sections in high-density metropolitan WDM networks," *IEEE Photon. Technol. Lett.*, vol. 14, no. 7, pp. 1013–1015, Jul. 2002.

[2] A. H. H. Tan, "Super PON-a fiber to the home cable network for CATV and POTS/ISDN/VOD as economical as a coaxial cable network," *J. Lightw. Technol.*, vol. 15, no. 2, pp. 213–218, Feb. 1997.

[3] X. P. Mao, G. E. Bodeep, R. W. Tkach, A. R. Chraplyvy, T. E. Darcie, and R. M. Dorosier, "Brillouin scattering in externally modulated lightwave AM-VSB CATV transmission systems," *IEEE Photon. Technol. Lett.*, vol. 4, no. 3, pp. 287–289, Mar. 1992.

[4] S. Radic, C. J. McKinstrie, R. M. Jopson, J. C. Centanni, and A. R. Chraplyvy, "All-optical regeneration in one- and two-pump parametric amplifiers using highly nonlinear optical fiber," *IEEE Photon. Technol. Lett.*, vol. 15, no. 7, pp. 957–959, Jul. 2003.

[5] T. Torounidis, H. Sunnerud, P. O. Hedekvist, and P. A. Andrekson, "40-Gb/s transmission using RZ-pulse source based on fiber optical parametric amplification," *IEEE Photon. Technol. Lett.*, vol. 15, no. 8, pp. 1159–1161, Aug. 2003.

[6] M. E. Marhic, K. K. Y. Wong, M. C. Ho, and L. G. Kazovsky, "92% pump depletion in a continuos-wave one-pump fiber-optical parametric amplifier," *Opt. Lett.*, vol. 26, no. 9, pp. 620–622, May 2001.

[7] J. M. Chavez Boggio, P. Dainese, F. Karlsson, and H. L. Fragnito, "Broadband 88% efficient two-pump fiber optical parametric amplifier," *IEEE Photon. Technol. Lett.*, vol. 15, no. 11, pp. 1528–1530, Nov. 2003.

[8] F. A. Callegari, J. M. Chavez Boggio, and H. L. Fragnito, "Spurious four-wave mixing in two-pump fiber-optical parametric amplifiers," *IEEE Photon. Technol. Lett.*, vol. 16, no. 2, pp. 434–436, Feb. 2004.

[9] S. K. Korotky, P. B Hansen, L. Eskildsen, and J. J. Veselka, "Efficient phase modulation scheme for suppressing stimulated Brillouin scattering," in *Tech. Dig. Int. Conf. Integrated Optics Optical Fiber Communications*, Hong Kong, 1995, vol. 2, pp. 110–111, Paper WD2-1.

[10] K. Shiraki, M. Ohashi, and M. Tateda, "Suppression of stimulated Brillouin scattering in a fibre by changing the core radius," *Electron. Lett.*, vol. 31, no. 8, pp. 668–669, Apr. 1995.

[11] K. Tsujikawa, K. Nakajima, Y. Miyajima, and M. Ohashi, "New SBS suppression fiber with uniform chromatic dispersion to enhance four-wave mixing," *IEEE Photon. Technol. Lett.*, vol. 10, no. 8, pp. 1139–1141, Aug. 1998.

[12] K. Shiraki, M. Ohashi, and M. Tateda, "SBS threshold of fiber with a Brillouin frequency shift distribution," *J. Lightw. Technol.*, vol. 14, no. 1, pp. 50–56, Jan. 1996.

[13] ——, "Performance of strain-free stimulated Brillouin scattering suppression fiber," *J. Lightw. Technol.*, vol. 14, no. 4, pp. 549–554, Apr. 1996.

[14] Y. Imai and N. Shimada, "Dependence of stimulated Brillouin scattering on temperature distribution in polarization-maintaining fibers," *IEEE Photon. Technol. Lett.*, vol. 5, no. 11, pp. 1335–1337, Nov. 1993.

[15] J. Hansryd, F. Dross, M. Westlund, P. A. Andrekson, and S. N. Knudsen, "Increase of the SBS threshold in a short highly nonlinear fiber by applying a temperature distribution," *J. Lightw. Technol.*, vol. 19, no. 11, pp. 1691–1697, Nov. 2001.

[16] N. Yoshizawa and T. Imai, "Stimulated Brillouin scattering suppression by means of applying strain distribution to fiber with cabling," *J. Lightw. Technol.*, vol. 11, no. 10, pp. 1518–1522, Oct. 1993.

[17] J. D. Marconi, J. M. Chavez Boggio, and H. L. Fragnito, "7.3 dB increase of the SBS threshold in an optical fiber by applying a strain distribution," presented at the Tech. Dig. Optical Fiber Communication Conf., Los Angeles, CA, 2004, Paper MF12.

[18] R. W. Boyd, *Nonlinear Optics*. San Diego, CA: Academic, 1992, pp. 325–349.

[19] A. L. Gaeta and R. W. Boyd, "Stochastic dynamics of stimulated Brillouin scattering in an optical fiber," *Phys. Rev. A*, vol. 44, no. 5, pp. 3205–3209, Nov. 1991.

[20] G. P. Agrawal, *Nonlinear Fiber Optics*. San Diego, CA: Academic, 1995, pp. 370–403.

[21] V. I. Kovalev and R. G. Harrison, "Waveguide-induced inhomogeneous spectral broadening of stimulated Brillouin scattering in optical fiber," *Opt. Lett.*, vol. 27, no. 22, pp. 2022–2024, Nov. 2002.

[22] M. Niklès, L. Thévenaz, and P. A. Robert, "Brillouin gain spectrum characterization in single-mode optical fibers," *J. Lightw. Technol.*, vol. 15, no. 10, pp. 1842–1851, Oct. 1997.

[23] T. Horiguchi, T. Kurashima, and M. Tateda, "Tensile strain dependence of Brillouin frequency shift in silica optical fibers," *IEEE Photon. Technol. Lett.*, vol. 1, no. 5, pp. 107–108, May 1989.

[24] J. M. Chavez Boggio, S. Tenenbaum, and H. L. Fragnito, "Four wave mixing induced changes in the noise spectrum in an optical fiber," in *Tech. Dig. Optical Fiber Communication Conf.*, Anaheim, CA, 2001, pp. WDD24-1–WDD24-4.

[25] ——, "Amplification of broadband noise pumped by two lasers in optical fibers," *J. Opt. Soc. Amer. B*, vol. 18, no. 10, pp. 1428–1435, Oct. 2001.

J. M. Chavez Boggio, photograph and biography not available at the time of publication.

J. D. Marconi, photograph and biography not available at the time of publication.

H. L. Fragnito, photograph and biography not available at the time of publication.